Myeloma cells contain high levels of inorganic polyphosphate which is associated with nucleolar transcription

Maria D. Jimenez-Nuñez,[1,3] David Moreno-Sanchez,[1,3] Laura Hernandez-Ruiz,[1,3] Alicia Benítez-Rondán,[1] Ana Ramos-Amaya,[1] Beatriz Rodríguez-Bayona,[1,2] Francisco Medina,[1] José Antonio Brieva,[1,2] and Felix A. Ruiz[1,3]

[1]Unidad de Investigación and [2]Servicio de Immunología, Hospital Universitario Puerta del Mar, Cádiz; and [3]Facultad de Medicina, Universidad de Cádiz, Cádiz, Spain

ABSTRACT

Background

In hematology there has recently been increasing interest in inorganic polyphosphate. This polymer accumulates in platelet granules and its functions include modulating various stages of blood coagulation, inducing angiogenesis, and provoking apoptosis of plasma cells. In this study we evaluated the characteristics of intracellular polyphosphate in myeloma cell lines, in primary myeloma cells from patients, and in other human B-cell populations from healthy donors.

Design and Methods

We have developed a novel flow cytometric method for detecting levels of polyphosphate in cell populations. We also used confocal microscopy and enzymatic analysis to study polyphosphate localization and characteristics.

Results

We found that myeloma plasma cells contain higher levels of intracellular polyphosphate than normal plasma cells and other B-cell populations. Localization experiments indicated that high levels of polyphosphate accumulate in the nucleolus of myeloma cells. As the principal function of the nucleolus involves transcription of ribosomal DNA genes, we found changes in the cellular distribution of polyphosphate after the inhibition of nucleolar transcription. In addition, we found that RNA polymerase I activity, responsible for transcription in the nucleolus, is also modulated by polyphosphate, in a dose-dependent manner.

Conclusions

Our results show an unusually high accumulation of polyphosphate in the nucleoli of myeloma cells and a functional relationship of this polymer with nucleolar transcription.

Key words: polyphosphate, primary myeloma cells, B-cell populations, myeloma cell lines, nucleolus, nucleolar transcription, RNA polymerase I.

Introduction

Myeloma cells (MC) are a malignant transformation of plasma cells, the last stage in B-cell differentiation. MC proliferate in patients with multiple myeloma, a common and still incurable disease characterized by osteolytic bone lesions, hypercalcemia, renal insufficiency, and anemia.[1] A better understanding of the mechanisms that regulate MC proliferation is urgently needed for the development of more efficient drugs for the management of patients with multiple myeloma. In general, cell proliferation in eukaryotes is accompanied by increased ribosome biogenesis, in which transcription of most ribosomal RNA by RNA polymerase I (RNA pol I) in the nucleolus is a key process.[2] The involvement of RNA pol I in promoting cell proliferation makes it an attractive target for the treatment of cancer.[3]

Inorganic polyphosphate (polyP) is a linear polymer formed by phosphate (P_i) residues linked by ATP-like bonds, and is present in all cells studied from early in evolution.[4] PolyP has been studied very extensively in prokaryotes and unicellular eukaryotes, in which it accumulates in acidocalcisomes,[5] and is involved in stress responses and virulence.[4] Since our discovery that polyP is abundant and released by activated platelets,[6] there has been increasing interest in this polyanion in hematology. It has been found that released extracellular polyP modulates blood coagulation *in vitro*[7] and *in vivo*,[8] increases vascular permeability,[8] enhances fibrin clot structure,[9,10] promotes the inhibitory effect of factor VII activating protease on vascular smooth muscle cell proliferation,[11] and induces apoptosis in plasma cells and MC.[12]

In platelets, intracellular polyP is localized principally in dense granules (which are similar to acidocalcisomes),[6] and this characteristic has been used to diagnose δ-storage pool diseases.[13] However, the distribution and functions of intracellular polyP in blood cells other than platelets are poorly understood.[4]

In this study we investigated the distribution and characteristics of intracellular polyP in MC cell lines, and MC from patients with multiple myeloma, using enzymatic assays, flow cytometry, and confocal microscopy.

Design and Methods

Reagents

RPMI 1640 culture medium, Dulbecco's modified eagle's medium (DMEM), L-glutamine, fetal calf serum, penicillin and streptomycin were purchased from Gibco BRL Life Technologies (Paisley, Scotland). 4',6-Diamidino-2-phenylindole (DAPI), actinomycin D, α-amanitin, $polyP_{25}$, $polyP_{65}$, Sephadex G25, toluidine blue, and mouse monoclonal antibodies against B23 (nucleophosmin) were purchased from Sigma Chemicals Co. (St. Louis, MO, USA). Mouse monoclonal antibodies against fibrillarin were purchased from Abcam (Cambridge, UK). Rabbit polyclonal antibodies against PAF49/CAST (a subunit of human RNA pol I) were purchased from Bethyl Laboratories (Montgomery, TX, USA). Alexa647-labeled anti-rabbit, and Alexa647-labeled anti-mouse IgG were from Molecular Probes (Eugene, OR, USA). Allophycocyanin-labeled monoclonal antibodies against CD19, fluorescein isothiocyanate-labeled monoclonal antibodies against CD20, and phycoerythrin-labeled monoclonal antibodies against CD38 were purchased from Becton Dickinson (San Jose, CA, USA). Allophycocyanin-labeled monoclonal antibodies against CD138 were from Miltenyi Biotec GmbH (Gladbach, Germany).

Escherichia coli strain CA38 pTrcPPX1 was kindly provided by Prof. Arthur Kornberg (Stanford University School of Medicine, CA, USA). All other reagents were of analytical grade.

Cell lines and cell cultures

Human myeloma cell lines (HMCL) were obtained from the European Collection of Cell Cultures (ECACC, London, UK), which verified the identity of all cell lines by DNA profiling (www.hpacultures.org.uk). HMCL were grown in RPMI 1640 medium (U266, ECACC No. 85051003, and NCI-H929, ECACC No. 95050415) or DMEM (RPMI-8226 cell line, ECACC No. 87012702), supplemented with 10% fetal calf serum, 10 mM glutamine, 100 IU/mL penicillin, and 100 μg/mL streptomycin.

Preparation of bone marrow mononuclear cells and isolation of tonsil B cells

Material remaining from bone marrow aspirates of patients after the diagnosis of multiple myeloma was used. Bone marrow mononuclear cells were obtained by Ficoll/Hypaque density-gradient centrifugation as previously reported.[14] CD138+ cells (which were 97.9% myeloma cells) were isolated from the bone marrow mononuclear cells by immunomagnetic selection, as described elsewhere.[14] Tonsils were obtained from subjects undergoing tonsillectomy for chronic tonsillitis. Tonsil B cells were isolated by mechanical disaggregation and T-cell depletion, as previously described.[14] This study was approved by the institutional review board (Ethics Committee). Informed consent was obtained in accordance with the Declaration of Helsinki.

Total polyphosphate isolation, polyphosphate measurements, and urea-polyacrylamide gel analysis

Total polyP was isolated as described by Kumble and Kornberg.[15] The procedure includes incubation with saturating RNAase and DNAase, and subsequent extractions with phenol/chloroform. Final concentrations of polyP were measured using purified recombinant yeast exopolyphosphatase (*scPPX1*), as described previously.[16] In all experiments described here, polyP concentrations are expressed in terms of their phosphate residues (P_i). To estimate polyP concentrations, we used cell volume data from measurements previously described in a murine MC line,[17] whose cells have an average radius similar to U266 MC. Extracted total polyP was analyzed in a 6% urea-polyacrylamide gel.[6]

Flow cytometry analysis

Flow activated cell sorting (FACS) analysis was performed on a FACScalibur cytometer (Becton Dickinson). Cell analysis was performed with CELLQUEST software (Becton Dickinson). Green fluorescence (fluorescein isothiocyanate, FL1), red/orange fluorescence (phycoerythrin and propidium iodide, FL2), red fluorescence (allophycocyanin, FL4), were collected with 530/30 nm, 585/42 nm, and 661/16 nm bandpass filters respectively. For analysis of DAPI-polyP fluorescence, cells were fixed with 4% paraformaldehyde in phosphate-buffered saline for 30 min, washed twice and resuspended with 0.9% NaCl. Then, 1 mg/mL of DAPI, or a similar volume of water, was added. A final concentration of 160 μg/mL of DAPI was used. Fluorescence was collected with a 670 long-pass filter (FL3). Data from 10,000 cells per sample were collected.

Polyphosphate localization and immunostaining by fluorescence confocal microscopy

Fluorescence localization in the samples was visualized and recorded using a laser TCS-SL confocal imaging system (Leica Microsystems). For investigations of polyP localization using DAPI, washed cells were fixed with 4% paraformaldehyde in

phosphate-buffered saline for 30 min. The cells were then washed twice and resuspended with phosphate-buffered saline, and 1 mg/mL of DAPI was added. Samples were mounted on slides and observed under a confocal microscope (excitation: 458 nm, emission: 530-570 nm). Additional investigations of polyP localization on U266 MC were performed using the recombinant polyP-binding domain (PPBD) of *E. coli* PPX linked to an Xpress epitope tag.[18] Explanations of the method used for PPBD labeling are given in the legend to *Online Supplementary Figure S2B*. The localization of other proteins was determined by immunostaining, as also described in the legend to *Online Supplementary Figure S2B*, but using 1/50 dilutions of primary-specific antibodies and 1/100 dilutions of labeled secondary antibodies (Alexa647-labeled anti-rabbit or Alexa647-labeled anti-mouse IgG). For polyP co-localization, 0.6 mg/mL of DAPI was added to the antibody-stained coverslips before observation by a confocal microscope, as described above.

Actinomycin D treatment of U266 myeloma cells

Cells were incubated in 5 µg/mL of actinomycin D diluted in culture media supplemented with 10% fetal calf serum (5×10^5 cells/mL) at 37°C for 3 h. Cells were then fixed and stained with DAPI for polyP localization by confocal microscopy as described above.

RNA polymerase I activity

Nucleoli were isolated as previously described.[19] Aliquots of MC nucleolar fractions (5 µL) were analyzed for RNA pol I activity in a non-specific transcription assay with sheared calf thymus DNA templates, 0.1 mg/mL α-amanitin, ATP, GTP, UTP, CTP, and [α-^{32}P] CTP as described before.[20] Different concentrations of polyP$_{65}$ (0 to 1 mM) were added to the transcription assay.

Results

Polyphosphate is present in myeloma cell lines

We measured levels of polyP in the U266 HMCL using purified recombinant yeast exopolyphosphatase (*scPPX1*). PolyP levels of 91.8±5.7 pmol/10^6 cells were detected in U266 MC (n=6). The volume in MC has been estimated to be 1.4 pL/cell,[17] and therefore the measured polyP concentration was around 65 µM. Using this method, we also measured polyP in total human peripheral blood mononuclear cells, obtaining levels of 4.5 ±2 pmol polyP/10^6 cells (n=3).

We also investigated the localization of polyP in HMCL by using DAPI. The method of polyP detection using DAPI was first described in the early 1980s.[21] Since that time, this procedure has been used in several studies (some examples are references:[6,8,13,16,22-25]). Emission fluorescence of DAPI shifts to longer wavelengths in the presence of polyP: this change is specific for polyP and is not produced by PPi, DNA, or other anions.[23,25] In U266 MC, we found differential fluorescent labeling with DAPI when settings for DNA or polyP detection were used (*Online Supplementary Figure S1A*). We have also found different patterns of labeling using a specific method for RNA detection (*Online Supplementary Figure S1B*).

In U266 cells (Figure 1A), and in other HMCL (*Online Supplementary Figure S2A*), we detected polyP in intranuclear structures and in the cytoplasm. Using a microscope image analysis program (Leica Confocal Software, Leica Microsystems), we determined that the signal intensity in the cytoplasm was 4-5 times lower than that in the

intranuclear structures, suggesting that polyP accumulates in the nucleus (*Online Supplementary Figure S2D*). In general, each cell had one to three of these polyP-rich structures with an average diameter of 1.4 µm, and all were located inside the nucleus (Figure 1A).

U266 MC were also stained using a protein that contains a PPBD[18] (*Online Supplementary Figure S2B*), or with toluidine blue, a polyP-detecting dye[26] (*Online Supplementary Figure S2C*). In all cases, U266 MC showed staining in intranuclear structures and also in the cytoplasm. However, the signal from the intranuclear structures was less pronounced with the PPBD protein staining method than with the DAPI method, with the intensity of the signals observed between intranucleolar and cytoplasmic areas being similar (*Online Supplementary Figure S2B*). No staining was detected in HMCL when DAPI, PPBD protein, or toluidine blue was omitted (*results not shown*).

The presence of polyP in HMCL was further demonstrated using permeabilized U266 cells. The labeling of rounded structures inside the nucleus decreased slightly after treatment with yeast exopolyphosphatase (*scPPX1*) (*Online Supplementary Figure S3*). The enzyme *scPPX1* can be inhibited by negative-charged polymers, such as heparin[27] or RNA (*results not shown*). We, therefore, tested DAPI labeling of polyP in U266 permeabilized cells after treatment with *scPPX1* and RNAase (*Online Supplementary Figure S3*). Treatment with both enzymes together resulted in the complete abolition of labeling with DAPI, but the addition of RNA$_{ase}$ alone did not produce any changes (*Online Supplementary Figure S3*).

In order to resolve the polymer size distribution, total polyP extracted from U266 cells was separated by 6% urea-polyacyrlamide gel electrophoresis and stained with toluidine blue (Figure 1B). The principal class of polyP detected in the MC samples was a little longer than the polyP standard of 65 residues on average (Figure 1B). These polymers extracted from U266 cells were degraded by *scPPX1* but not by heparinase, as occurs with commercial polyP standards (*Online Supplementary Figure S4*).

We developed a flow cytometry method to analyze the contents of intracellular polyP in cell populations using DAPI (Figure 1C). In cells[16] and human tissues,[28] DAPI-polyP complexes emit fluorescence exclusively above 580 nm. We, therefore, determined differences in fluorescence in the absence and presence of DAPI in the FL3 channel of the flow cytometer (filter 670LP), in combination with myeloma-specific surface marker labeling (CD138).

We tested the specificity of this flow cytometry method for polyP determination. DAPI fluorescence in the FL3 channel of the flow cytometer decreased in permeabilized U266 HMCL treated with *scPPX1* (*Online Supplementary Figure S5A*). In addition, fluorescence emission profiles of DAPI-labeled U266 MC, excited with a wavelength similar to that used in flow cytometry (488 nm), were similar to the emissions previously reported for pure polyP (*Online Supplementary Figure S5B*). Moreover, the DAPI concentration used (160 µg/mL) was optimal for this assay, as determined in U266 HMCL (*Online Supplementary Figure S6*).

U266 HMCL had a basal mean fluorescence intensity (MFI) of 3.5±1.1, and this fluorescence increased with the addition of DAPI up to 47.8±15.6 (n=6) (Figure 1C). Changes in the specific fluorescence associated with the formation of DAPI-polyP complexes were quantified as the ΔMFI in the presence and absence of DAPI, and this value was 44.5±16.3 for U266 HMCL.
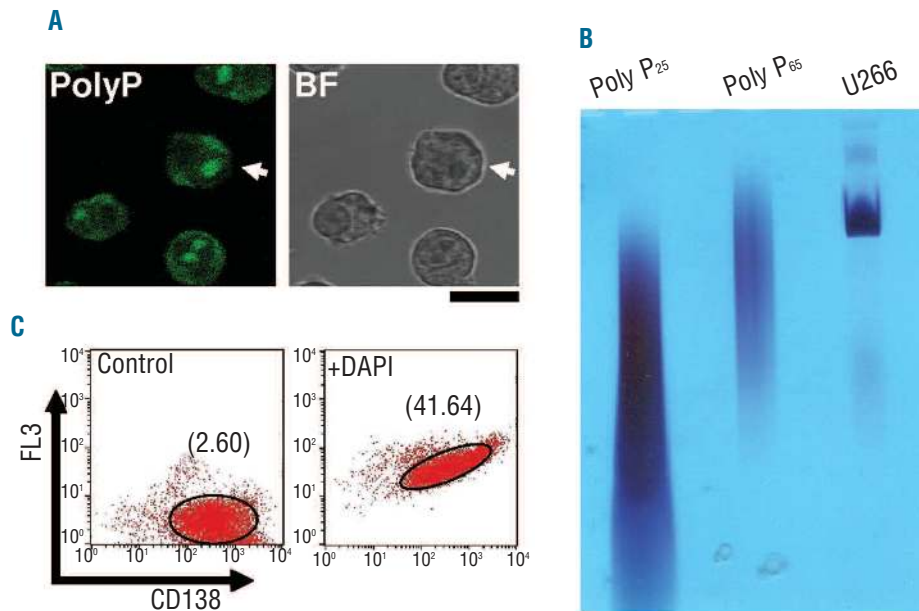
Figure 1. Polyphosphate is present in human myeloma cell lines (HMCL). (A) Localization of cellular polyphosphate (polyP) in the U266 MC line. Fixed cells were treated with DAPI, and specific polyP labeling was determined by confocal fluorescence microscopy (PolyP). The corresponding bright field image is shown (BF). Bar: 10 μm. PolyP cellular distributions in other HMCL (NCI and RPMI) are shown in *Online Supplementary Figure S2A*. The fluorescence intensity profile of the cell indicated with an arrow is shown in *Online Supplementary Figure S2B*. **(B)** Size analysis of polyP from U266 MC. Extracted polyP was separated by 6% urea-polyacrylamide gel electrophoresis (U266) and the gel was stained with toluidine blue to visualize polyP. PolyP$_{25}$ and polyP$_{65}$ were used as standards. **(C)** Flow cytometry analysis of U266 cells labeled with anti-CD138 phycoerythrin antibodies in the absence (Control) and presence of DAPI (+DAPI). The geometric mean fluorescence intensities (MFI) in the FL3 channel of the flow cytometer are indicated. The results of a representative experiment of six are shown.

Polyphosphate in primary myeloma cells

We studied the localization of polyP, using confocal microscopy, in primary MC isolated by specific immunoselection following extraction from bone marrow samples from patients with multiple myeloma (Figure 2A). The distribution of polyP in these primary MC was similar to that obtained in MC lines, with the presence of intense, corresponding spherical polyP-rich structures inside the nucleus (Figure 2A).

We next analyzed the whole population of bone marrow mononuclear cells from multiple myeloma patients by flow cytometry, using myeloma-specific surface marker labeling (CD138) in addition to the polyP-DAPI staining (Figure 2B,C). As above, changes in the specific fluorescence associated with the formation of DAPI-polyP complexes were quantified as the ΔMFI, in the FL3 channel, in the presence and absence of DAPI (Figure 2C). The change in MFI was three times greater in primary MC (CD138$^+$ cells) than in non-myeloma bone marrow mononuclear cells (CD138$^-$ cells) (Figure 2C). ΔMFI values in primary MC and U266 HMCL were not significantly different.

Polyphosphate in normal plasma cells and other B-cell populations

When isolated tonsil B cells are stained for CD20 and CD38 expression, three different populations can be distinguished by flow cytometry: normal plasma cells (CD38^{high}), germinal center B cells (CD38$^+$ CD20^{++}) and mantle zone B cells (CD38$^-$ CD20$^+$)[29] (Figure 3A). In these three populations we measured the changes in fluorescence generated by the formation of DAPI-polyP complexes (Figure 3B, C). The values of ΔMFI (in the FL3 channel) in the presence and absence of DAPI, were very low in normal plasma cells and in the other B-cell populations (Figures 2B and 3C). These ΔMFI values were similar for all B-cell populations but significantly different in comparison with the values obtained for primary MC or HMCL (Figures 2B and 3C).

Analysis by confocal microscopy

Using confocal microscopy, we confirmed that the polyP-rich structures inside the nucleus of MC are nucleoli (Figure 4). We found a strong co-localization between polyP and fibrillarin, a well-known nucleolar protein marker[30] (Figure 4A).

Additionally, we carried out an analysis of polyP localization within the nucleolus (Figure 4B), using the subnucleolar markers B23 (granular component), RNA pol I (fibrillar center), and fibrillarin (dense fibrillar component).[30] (Figure 4B,C). We found that polyP co-localized with fibrillarin and co-localized partially with RNA pol I, suggesting that this polymer is accumulated in the nucleolar dense fibrillar component, and in the fibrillar center as well (Figure 4B,C).

Changes in polyphosphate localization after inhibition of transcription

The principal function of the nucleolus is the biogenesis of ribosome subunits, a process that requires the transcription of rDNA genes. To study whether polyP could be associated with this process, we tested changes in polyP content and distribution after inhibition of the transcription of MC (Figure 5). A brief treatment of U226 HMCL with actinomycin D, which specifically inhibits transcription by RNA polymerases,[19,31,32] produced clear decreases in nucleolar polyP (Figure 5A,B) and in total cellular polyP levels (Figure 5D). In parallel, small polyP-rich structures appeared in the cytoplasm after the actinomycin D treatment (Figure 5A,C).

We also studied polyP distribution in cells treated with MG132, a proteasome inhibitor that affects nucleolar morphology without inhibitimg RNA polymerase activity.[33] Three hours of treatment with 10 μM of MG132 changed nucleoli morphology to more elongated shapes, but did not produce a reduction in nucleolar polyP levels or any development of cytoplasmatic polyP structures (*results not shown*).

### Polyphosphate modulates myeloma cell RNA polymerase I activity

RNA polymerase activity within the nucleolus is affected exclusively by RNA pol I. We, therefore, tested the effect of the addition of exogenous polyP on the total activity of RNA pol I in enriched nucleolar fractions, using a non-specific transcription assay. The addition of synthetic polyP inhibited total RNA pol I activity in a dose-dependent fashion (Figure 6). The maximum inhibition of total RNA pol I activity was around 50%, and this level was reached with the addition of 100 μM polyP (Figure 6).

Discussion

In this work we found the presence of particularly high levels of intracellular polyP in primary MC and in HMCL,

in comparison with levels in normal primary plasma cells, B cells and non-myeloma boen marrow mononuclear cells (Figures 1-3). In this analysis, we used a flow cytometry method to determine relative cellular polyP accumulation in different populations of human bone marrow mononuclear cells. Several authors have described similar approaches for detecting polyP in bacteria populations[34-37] but, to our knowledge, this is the first time that this technique has been applied in human cells to detect polyP.

We employed, principally, a widely-used method for the detection of polyP with DAPI.[6,8,13,16,21-25] The other staining method for polyP detection (PPBD protein) showed a less pronounced polyP signal in the nucleoli (*Online Supplementary Figure 2B*). It has previously been reported that DNA and RNA inhibit the binding of PPBD to polyP.[18] Staining with PPBD protein could, therefore, underestimate the existing amount of polyP within RNA-rich
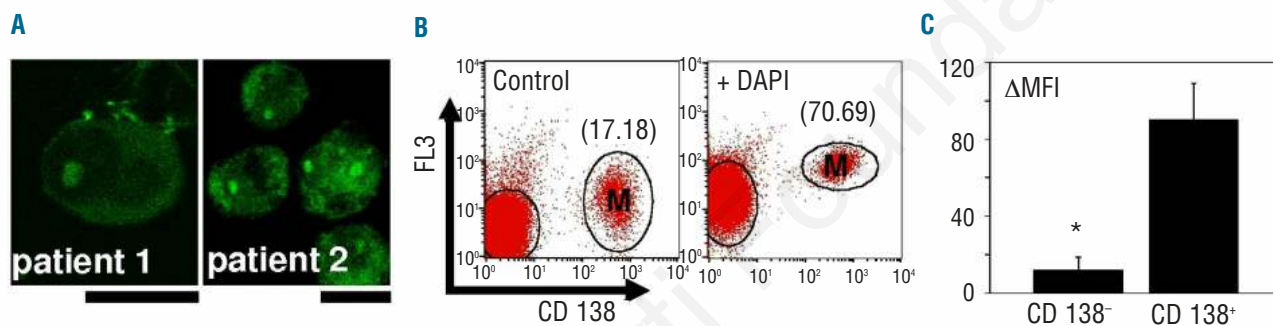
Figure 2. PolyP in primary MC. (**A**) Confocal fluorescence microscopy of fixed human myeloma cells after specific polyP labeling with DAPI. Cells were isolated, by CD138-dependent immunomagnetic selection, from the bone marrow of six patients with multiple myeloma (MM). Bar: 10 μm. Representative pictures are shown (patient 1 and patient 2). (**B**) Flow cytometry analysis of isolated bone marrow mononuclear cells, from MM patients. Fixed cells, labeled with anti-CD138 phycoerythrin antibodies, were incubated in the absence (Control) and presence of DAPI (+DAPI), as described in the legend of Figure 1. The geometric mean fluorescence intensities (MFI), in the FL3 channel of the flow cytometer, are indicated for the MC (CD 138⁺). Measurements for one representative sample of six are shown. (**C**) Quantification of the differences in the geometric MFI (ΔMFI), in the FL3 channel, after the addition of DAPI. MC (CD 138⁺) and other mononuclear cells (CD138⁻) from bone marrow samples were analyzed as described in panel (**B**). Results represent the mean ± SD of the measurements made in the samples of six MM patients. The asterisk indicates a significant difference in comparison with primary MC, as determined by the t test (*P*<0.05).
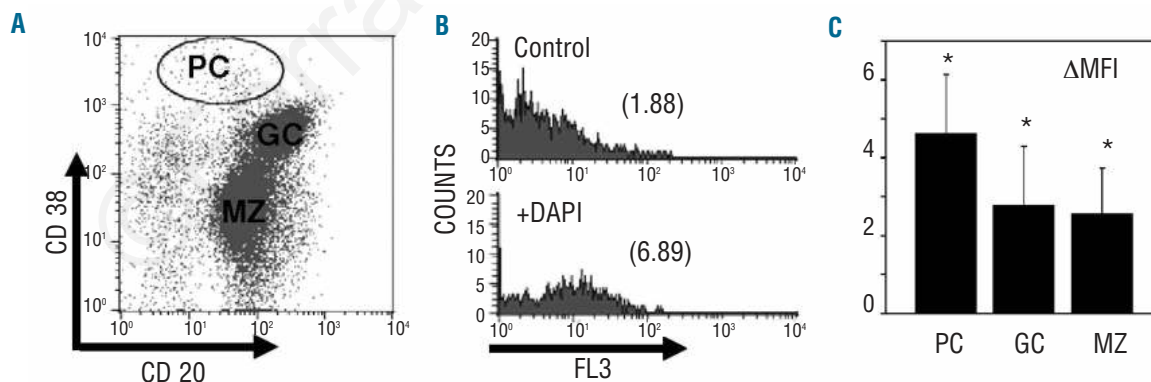
Figure 3. PolyP levels are lower in primary normal plasma cells and other B-cell populations. (**A**) Flow cytometry analysis of B-cell populations isolated from human tonsils. Cells were analyzed after simultaneous labeling with anti-CD38 phycoerythrin and anti-CD20 fluoroscein isothiocyanate antibodies. The dot plot represents a typical pattern of CD20/CD38 expression in human tonsil B cells, in which different subsets are indicated: plasma cells (PC), germinal center (GC) and mantle zone (MZ) B cells. The measurements from one representative sample of five are shown. (**B**) Fixed samples of labeled tonsil B cells, as described in panel (**A**), were incubated in the absence (Control) or presence of DAPI (+DAPI). Cell fluorescence of gated PC in the FL3 channel was determined. The geometric mean fluorescence intensities (MFI) are indicated. The measurements from one representative sample of five are shown. (**C**) Differences in the geometric MFI (ΔMFI) in the FL3 channel, after the addition of DAPI, for the different B-cell subsets: plasma cells (PC), germinal center (GC) and mantle zone (MZ) B cells. Results represent the mean ± SD of the measurements made in the samples of five patients. The asterisk indicates significant differences in comparison with data from U266 HMCL and primary MC, determined by the t test (*P*<0.05).

organelles, such as the nucleoli.

Using purified recombinant yeast exopolyphosphatase (*scPPX1*), we were able to measure levels of 65 μM of polyP in the U266 HMCL. This value is 6 to 20 times higher than the polyP concentrations found in total human peripheral blood mononuclear cells[38] (see *Results* section), but 15 times lower than the polyP concentrations described by us in human platelets.[6]

We have also discovered that polyP polymers of approximately 75-80 P_i residues are the main intracellular type of polyP found in MC (Figure 1B). PolyP polymers of this size are frequently found in mammalian cell signaling, and these molecules have been reported to stimulate mTOR kinase in mammary cancer cells,[39] to interact with fibroblast growth factor,[40] to be released by activated platelets,[6] and to modulate blood coagulation.[7]

We have previously described that the addition of mil-limolar concentrations of extracellular polyP induces apoptosis specifically in MC and plasma cells.[12] However, in the present work, we studied intracellular polyP in MC. Using specific enzymatic procedures, we estimated that the intracellular concentration of polyP in MC is in the micromolar range. In accordance with these results and others (unpublished data from Moreno-Sanchez and Ruiz), we believe that MC could respond differently to polyP depending on whether its location is intra- or extra-cellular.

We have also described here that intracellular polyP is mostly accumulated within the nucleolus of MC. Confocal microscopy experiments showed co-localization of polyP and nucleolar markers (Figure 4). PolyP had previously been found in various other subcellular compartments, including mitochondria,[15] platelet dense granules,[6] and acidocalcisomes of unicellular organisms.[5] Elevated
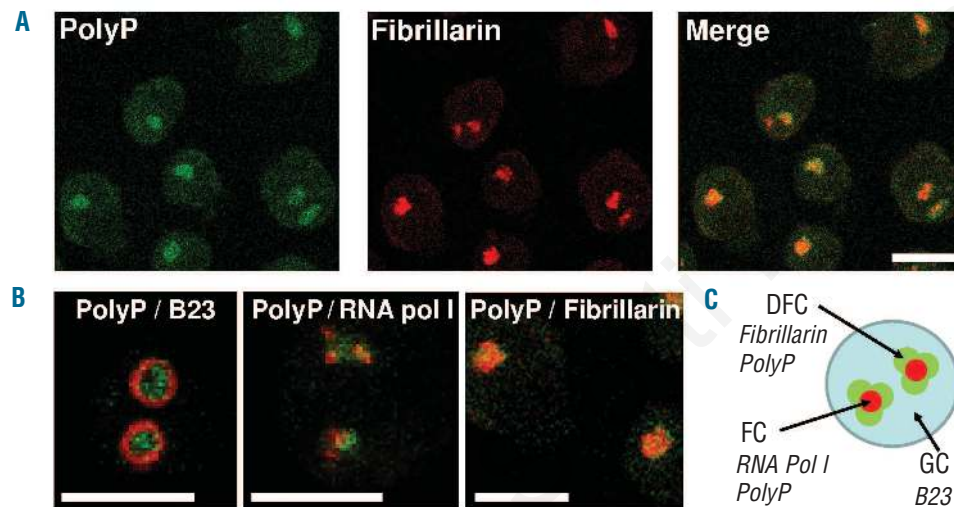
Figure 4. Confocal immunofluorescence analysis in U266 MC. (A) The figure shows the colocalization of polyP and fibrillarin (nucleolar marker). (B) Analysis of subnucleolar markers and polyP localization: the figure shows merged images of the localization of polyP (green) and the following nucleolar proteins (in red): B23 (granular component), RNA pol I (fibrillar center), and fibrillarin (dense fibrillar component). Bars: 10 μm. Representative experiments are shown (n=3). (C) Descriptive scheme of polyP distribution within the nucleolus: in accordance with the results shown in 4B, a model describing polyP distribution in the subnucleolar compartments was devised. GC: granular component, FC: fibrillar center, DFC: dense fibrillar component. (Adapted from Lam *et al*.[30]).
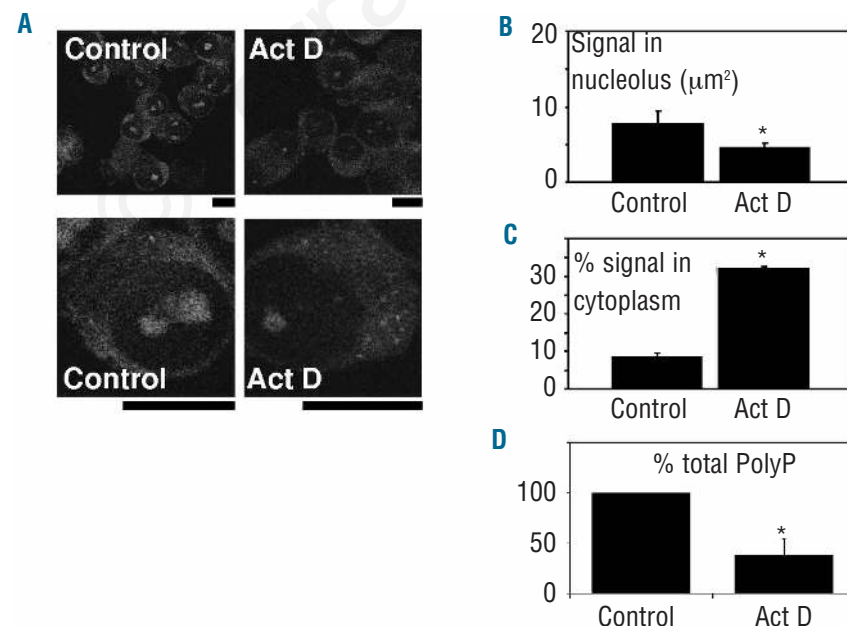
Figure 5. Movement of polyP in MC induced by inhibition of nucleolar transcription. (A) U266 HMCL was incubated in the absence (Control) or presence (Act D) of actinomycin D (5 μg/mL). PolyP cellular distribution was then determined by specific labeling using DAPI and confocal microscopy. Lower panels show images at higher magnification. Bars: 10 μm. Results from a representative experiment of three are shown. (B) Quantification of polyP labeling in the nucleolar area of control and Act D-treated cells. (C) Quantification of control and Act D-treated cells with polyP vacuoles inside the cytoplasm. (D) Relative levels of total polyP, measured by sc*PPX1*, of control and Act D-treated cells. Results in panels B, C and D represent the mean ± SD from three separate experiments. Asterisks indicate the results that were significantly different, by the t test (*P*<0.05).

concentrations of polyP in rat liver nuclei, have been reported,[15] but the distribution of the polyP within the organelle was not reported.

In fact, nucleolar polyP localization appears to be specific for MC. PolyP distribution has been investigated in several other cell lines and primary cultures, including hepatic carcinoma, embryonic kidney, myoblasts, astrocytes and neurons.[22,23] In those cells, the polyP signal was much weaker in the nuclear region, and the prevalent finding was a diffuse signal from the surrounding zone[22]

Inhibition of transcription, following treatment with actinomycin D, induced the polyP to move from the nucleoli to the cytoplasm in MC (Figure 5). It is well known that actinomycin D treatment causes several factors to leave the nucleoli, including ribosomal proteins, exosome components and RNA pol I.[19] We believe that the association of polyP with the nucleolus could be dependent on ribosome subunit synthesis, in accordance with what has been proposed for those other factors.

Furthermore, the demonstration that polyP modulates RNA pol I in MC (Figure 6), is the first direct association found between intracellular polyP and transcriptional activity in a mammalian cell. In bacteria, it has been shown that polyP interacts with RNA polymerase enzymes modulating their transcriptional activity according to the culture growth phase.[41] PolyP also induces transcription of *rpoS*, a bacterial gene that encodes a stationary phase-specific RNA polymerase.[42]

We propose that polyP could be a new factor associated with the specificity of RNA pol I transcription for particular rRNA genes in MC. It has been described previously that, even in exponentially growing cells, only half of the available rRNA genes are actively transcribed.[2] Chromatin and several regulatory factors are involved in the control of RNA pol I transcription for specific rRNA genes, and they also enable changes in enzyme specificity as a response to alterations in the cellular environment.[43] However, additional studies are necessary to understand the mechanisms through which polyP modulates the activity of RNA pol I in MC.

In addition, we believe that polyP organization could also be involved in the regulation of enzymatic activities in the various subcompartments within the nucleolus. PolyP is localized mostly in the nucleolar dense fibrillar component (Figure 4B,C), where transcription levels are low, and pre-rRNA transcripys are sliced and modified.[44]

It has been reported that polyP plays several other roles controlling gene expression in microorganisms.[4] In *E. coli*, it has been demonstrated that polyP is a potent inhibitor of the degradosome-dependent degradation of mRNA[45] and a promoter of ribosomal[46] and nucleoid[47] protein degradation by activating Lon protease; it also assists in
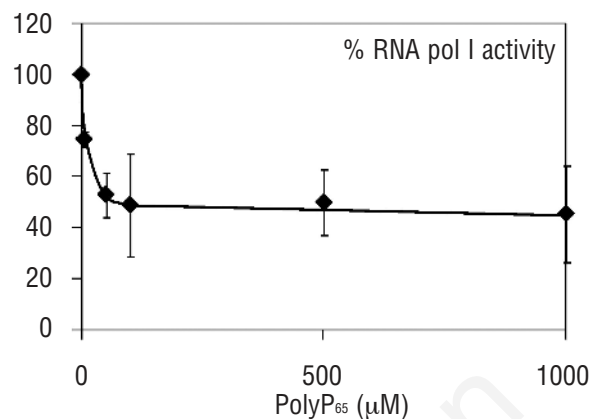
Figure 6. Effect of polyP addition on *in vitro* transcription by RNA polymerase I (RNA pol I). Aliquots of the nucleolar fraction from U266 HMCL were analyzed for RNA pol I transcription activity in a non-specific transcription assay. $PolyP_{65}$ was added in the assay at the indicated concentrations. Results from a representative experiment performed in triplicate is shown, with the standard deviation of the data indicated by error bars.

the fidelity of protein translation by its interaction with ribosomes.[48] In yeast, polyP interacts and inhibits poly(A) polymerase activities.[49,50] Therefore, new roles for intracellular polyP in regulating gene expression in MC, and in other mammalian cells, could emerge when these studies are taken further.

The particularly high concentrations of nucleolar polyP found in human MC make this polymer of increasing interest for a better understanding of MC biology. The enzymes involved in polyP metabolism in MC are still unknown, but their potential for controlling MC proliferation makes them an attractive focus for prospective studies. Currently, MC from patients of different molecular subgroups[51] or with different stages of the disease[52] could be excellent models for studying myeloma polyP metabolism.

Authorship and Disclosures

References

1. Kyle RA, Rajkumar SV. Multiple myeloma. Blood. 2008;111(6):2962-72.
2. Russell J, Zomerdijk JC. RNA-polymerase-I-directed rDNA transcription, life and works. Trends Biochem Sci. 2005;30(2):87-96.
3. Drygin D, Rice WG, Grummt I. The RNA polymerase I transcription machinery: an emerging target for the treatment of cancer. Annu Rev Pharmacol Toxicol. 2010;50:131-56.
4. Rao NN, Gomez-Garcia MR, Kornberg A. Inorganic polyphosphate: essential for growth and survival. Annu Rev Biochem. 2009;78:605-47.
5. Docampo R, de Souza W, Miranda K, Rohloff P, Moreno SN. Acidocalcisomes - conserved from bacteria to man. Nat Rev Microbiol. 2005;3(3):251-61.
6. Ruiz FA, Lea CR, Oldfield E, Docampo R. Human platelet dense granules contain polyphosphate and are similar to acidocalcisomes of bacteria and unicellular eukaryotes. J Biol Chem. 2004;279(43):44250-7.
7. Smith SA, Mutch NJ, Baskar D, Rohloff P, Docampo R, Morrissey JH. Polyphosphate modulates blood coagulation and fibrinolysis. Proc Natl Acad Sci USA. 2006;103(4):903-8.
8. Muller F, Mutch NJ, Schenk WA, Smith SA, Esterl L, Spronk HM, et al. Platelet polyphos-

phates are proinflammatory and procoagulant mediators in vivo. Cell. 2009;139(6): 1143-56.

9. Smith SA, Morrissey JH. Polyphosphate enhances fibrin clot structure. Blood. 2008; 112(7):2810-6.

10. Mutch NJ, Engel R, Uitte de Willige S, Philippou H, Ariens RA. Polyphosphate modifies the fibrin network and down-regulates fibrinolysis by attenuating binding of tPA and plasminogen to fibrin. Blood. 2010;115(19):3980-8.

11. Muhl L, Galuska SP, Oorni K, Hernandez-Ruiz L, Andrei-Selmer LC, Geyer R, et al. High negative charge-to-size ratio in polyphosphates and heparin regulates factor VII-activating protease. FEBS J. 2009;276 (17):4828-39.

12. Hernandez-Ruiz L, Gonzalez-Garcia I, Castro C, Brieva JA, Ruiz FA. Inorganic polyphosphate and specific induction of apoptosis in human plasma cells. Haematologica. 2006;91(9):1180-6.

13. Hernandez-Ruiz L, Saez-Benito A, Pujol-Moix N, Rodriguez-Martorell J, Ruiz FA. Platelet inorganic polyphosphate decreases in patients with delta storage pool disease. J Thromb Haemost. 2009;7(2):361-3.

14. Medina F, Segundo C, Campos-Caro A, Gonzalez-Garcia I, Brieva JA. The heterogeneity shown by human plasma cells from tonsil, blood, and bone marrow reveals graded stages of increasing maturity, but local profiles of adhesion molecule expression. Blood. 2002;99(6):2154-61.

15. Kumble KD, Kornberg A. Inorganic polyphosphate in mammalian cells and tissues. J Biol Chem. 1995;270(11):5818-22.

16. Ruiz FA, Rodrigues CO, Docampo R. Rapid changes in polyphosphate content within acidocalcisomes in response to cell growth, differentiation, and environmental stress in Trypanosoma cruzi. J Biol Chem. 2001; 276(28):26114-21.

17. Shirakashi R, Kostner CM, Muller KJ, Kurschner M, Zimmermann U, Sukhorukov VL. Intracellular delivery of trehalose into mammalian cells by electropermeabilization. J Membr Biol. 2002;189(1):45-54.

18. Saito K, Ohtomo R, Kuga-Uetake Y, Aono T, Saito M. Direct labeling of polyphosphate at the ultrastructural level in Saccharomyces cerevisiae by using the affinity of the polyphosphate binding domain of Escherichia coli exopolyphosphatase. Appl Environ Microbiol. 2005;71(10):5692-701.

19. Andersen JS, Lam YW, Leung AK, Ong SE, Lyon CE, Lamond AI, et al. Nucleolar proteome dynamics. Nature. 2005;433(7021):77-83.

20. Birch JL, Tan BC, Panov KI, Panova TB, Andersen JS, Owen-Hughes TA, et al. FACT facilitates chromatin transcription by RNA polymerases I and III. Embo J. 2009;28(7): 854-65.

21. Allan RA, Miller JJ. Influence of S-adenosylmethionine on DAPI-induced fluorescence of polyphosphate in the yeast vacuole. Can J Microbiol. 1980;26(8):912-20.

22. Abramov AY, Fraley C, Diao CT, Winkfein R, Colicos MA, Duchen MR, et al. Targeted polyphosphatase expression alters mitochondrial metabolism and inhibits calcium-dependent cell death. Proc Natl Acad Sci USA. 2007;104(46):18091-6.

23. Aschar-Sobbi R, Abramov AY, Diao C, Kargacin ME, Kargacin GJ, French RJ, et al. High sensitivity, quantitative measurements of polyphosphate using a new DAPI-based approach. J Fluoresc. 2008;18(5):859-66.

24. Ruiz FA, Marchesini N, Seufferheld M, Govindjee, Docampo R. The polyphosphate bodies of Chlamydomonas reinhardtii possess a proton-pumping pyrophosphatase and are similar to acidocalcisomes. J Biol Chem. 2001;276(49):46196-203.

25. Pavlov E, Aschar-Sobbi R, Campanella M, Turner RJ, Gomez-Garcia MR, Abramov AY. Inorganic polyphosphate and energy metabolism in mammalian cells. J Biol Chem. 2010;285(13):9420-8.

26. Lorenz B, Schroder HC. Methods for investigation of inorganic polyphosphates and polyphosphate-metabolizing enzymes. Prog Mol Subcell Biol. 1999;23:217-39.

27. Lichko LP, Andreeva NA, Kulakovskaya TV, Kulaev IS. Exopolyphosphatases of the yeast Saccharomyces cerevisiae. FEMS Yeast Res. 2003;3(3):233-8.

28. Omelon S, Georgiou J, Henneman ZJ, Wise LM, Sukhu B, Hunt T, et al. Control of vertebrate skeletal mineralization by polyphosphates. PLoS One. 2009;4(5):e5634.

29. Medina F, Segundo C, Brieva JA. Purification of human tonsil plasma cells: pre-enrichment step by immunomagnetic selection of CD31(+) cells. Cytometry. 2000;39(3):231-4.

30. Lam YW, Trinkle-Mulcahy L, Lamond AI. The nucleolus. J Cell Sci. 2005;118(Pt 7):1335-7.

31. Yao Z, Duan S, Hou D, Wang W, Wang G, Liu Y, et al. B23 acts as a nucleolar stress sensor and promotes cell survival through its dynamic interaction with hnRNPU and hnRNPA1. Oncogene. 2010;29(12):1821-34.

32. King EM, Holden NS, Gong W, Rider CF, Newton R. Inhibition of NF-kappaB-dependent transcription by MKP-1: transcriptional repression by glucocorticoids occurring via p38 MAPK. J Biol Chem. 2009;284(39): 26803-15.

33. Mattsson K, Pokrovskaja K, Kiss C, Klein G, Szekely L. Proteins associated with the promyelocytic leukemia gene product (PML)-containing nuclear body move to the nucleolus upon inhibition of proteasome-dependent protein degradation. Proc Natl Acad Sci USA. 2001;98(3):1012-7.

34. Gunther S, Trutnau M, Kleinsteuber S, Hause G, Bley T, Roske I, et al. Dynamics of polyphosphate-accumulating bacteria in wastewater treatment plant microbial communities detected via DAPI (4',6'-diamidino-2-phenylindole) and tetracycline labeling. Appl Environ Microbiol. 2009;75(7):2111-21.

35. Hung CH, Peccia J, Zilles JL, Noguera DR. Physical enrichment of polyphosphate-accumulating organisms in activated sludge. Water Environ Res. 2002;74(4):354-61.

36. Kawaharasaki M, Manome A, Kanagaw T, Nakamura K. Flow cytometric sorting and RFLP analysis of phosphate accumulating bacteria in an enhanced biological phosphorus removal system. Water Sci Technol. 2002;46(1-2):139-44.

37. Miyauchi R, Oki K, Aoi Y, Tsuneda S. Diversity of nitrite reductase genes in "Candidatus Accumulibacter phosphatis"-

dominated cultures enriched by flow-cytometric sorting. Appl Environ Microbiol. 2007;73(16):5331-7.

38. Lorenz B, Leuck J, Kohl D, Muller WE, Schroder HC. Anti-HIV-1 activity of inorganic polyphosphates. J Acquir Immune Defic Syndr Hum Retrovirol. 1997;14(2):110-8.

39. Wang L, Fraley CD, Faridi J, Kornberg A, Roth RA. Inorganic polyphosphate stimulates mammalian TOR, a kinase involved in the proliferation of mammary cancer cells. Proc Natl Acad Sci USA. 2003;100(20):11249-54.

40. Shiba T, Nishimura D, Kawazoe Y, Onodera Y, Tsutsumi K, Nakamura R, et al. Modulation of mitogenic activity of fibroblast growth factors by inorganic polyphosphate. J Biol Chem. 2003;278(29):26788-92.

41. Kusano S, Ishihama A. Functional interaction of Escherichia coli RNA polymerase with inorganic polyphosphate. Genes Cells. 1997;2(7):433-41.

42. Shiba T, Tsutsumi K, Yano H, Ihara Y, Kameda A, Tanaka K, et al. Inorganic polyphosphate and the induction of rpoS expression. Proc Natl Acad Sci USA. 1997; 94(21):11210-5.

43. Grummt I. Life on a planet of its own: regulation of RNA polymerase I transcription in the nucleolus. Genes Dev. 2003;17(14):1691-702.

44. Boisvert FM, van Koningsbruggen S, Navascues J, Lamond AI. The multifunctional nucleolus. Nat Rev Mol Cell Biol. 2007;8(7):574-85.

45. Blum E, Py B, Carpousis AJ, Higgins CF. Polyphosphate kinase is a component of the Escherichia coli RNA degradosome. Mol Microbiol. 1997;26(2):387-98.

46. Kuroda A, Nomura K, Ohtomo R, Kato J, Ikeda T, Takiguchi N, et al. Role of inorganic polyphosphate in promoting ribosomal protein degradation by the Lon protease in E. coli. Science. 2001;293(5530):705-8.

47. Kuroda A, Nomura K, Takiguchi N, Kato J, Ohtake H. Inorganic polyphosphate stimulates lon-mediated proteolysis of nucleoid proteins in Escherichia coli. Cell Mol Biol (Noisy-le-grand). 2006;52(4):23-9.

48. McInerney P, Mizutani T, Shiba T. Inorganic polyphosphate interacts with ribosomes and promotes translation fidelity in vitro and in vivo. Mol Microbiol. 2006;60(2):438-47.

49. Sillero MA, de Diego A, Silles E, Osorio H, Sillero A. Polyphosphates strongly inhibit the tRNA dependent synthesis of poly(A) catalyzed by poly(A) polymerase from Saccharomyces cerevisiae. FEBS Lett. 2003;550(1-3):41-5.

50. Holbein S, Freimoser FM, Werner TP, Wengi A, Dichtl B. Cordycepin-hypersensitive growth links elevated polyphosphate levels to inhibition of poly(A) polymerase in Saccharomyces cerevisiae. Nucleic Acids Res. 2008;36(2):353-63.

51. Broyl A, Hose D, Lokhorst H, de Knegt Y, Peeters J, Jauch A, et al. Gene expression profiling for molecular classification of multiple myeloma in newly diagnosed patients. Blood.116(14):2543-53.

52. Greipp PR, San Miguel J, Durie BG, Crowley JJ, Barlogie B, Blade J, et al. International staging system for multiple myeloma. J Clin Oncol. 2005;23(15):3412-20.